AD_____

GRANT NUMBER DAMD17-97-1-7067

TITLE: A High Resolution Scanning Slot X-Ray Imaging Detector for Digital Mammography

PRINCIPAL INVESTIGATOR: Zhenxue Jing

CONTRACTING ORGANIZATION: University of Florida
Gainesville, Florida 32611

REPORT DATE: June 1998

TYPE OF REPORT: Annual

PREPARED FOR: U.S. Army Medical Research and Materiel Command
Fort Detrick, Maryland 21702-5012

DISTRIBUTION STATEMENT: Approved for public release;
distribution unlimited

The views, opinions and/or findings contained in this report are those of the author(s) and should not be construed as an official Department of the Army position, policy or decision unless so designated by other documentation.

DTIC QUALITY INSPECTED 4

REPORT DOCUMENTATION PAGE

Form Approved
OMB No. 0704-0188

Public reporting burden for this collection of information is estimated to average 1 hour per response, including the time for reviewing instructions, searching existing data sources, gathering and maintaining the data needed, and completing and reviewing the collection of information. Send comments regarding this burden estimate or any other aspect of this collection of information, including suggestions for reducing this burden, to Washington Headquarters Services, Directorate for Information Operations and Reports, 1215 Jefferson Davis Highway, Suite 1204, Arlington, VA 22202-4302, and to the Office of Management and Budget, Paperwork Reduction Project (0704-0188), Washington, DC 20503.

1. AGENCY USE ONLY *(Leave blank)*	2. REPORT DATE	3. REPORT TYPE AND DATES COVERED
	June 1998	Annual (1Jun 97 - 31 May 98)

4. TITLE AND SUBTITLE

A High Resolution Scanning Slot X-Ray Imaging Detector for Digital Mammography

5. FUNDING NUMBERS

DAMD17-97-1-7067

6. AUTHOR(S)

Zhenxue Jing

7. PERFORMING ORGANIZATION NAME(S) AND ADDRESS(ES)

University of Florida
Gainesville, Florida 32611

8. PERFORMING ORGANIZATION REPORT NUMBER

9. SPONSORING / MONITORING AGENCY NAME(S) AND ADDRESS(ES)

U.S. Army Medical Research and Materiel Command
Fort Detrick, Maryland 21702-5012

10. SPONSORING / MONITORING AGENCY REPORT NUMBER

11. SUPPLEMENTARY NOTES

19990603 069

12a. DISTRIBUTION / AVAILABILITY STATEMENT

Approved for public release; distribution unlimited

12b. DISTRIBUTION CODE

13. ABSTRACT *(Maximum 200 words)*

There has been a major modification of the contents of the proposed work. The objective of this reported research is to develop new screen-film combinations which provide improved breast lesion and microcalcification sensitivity in dense fibroglandular tissue without compromising diagnostic sensitivity for the "average" breasts. The essential novelty of the approach lies in recognizing that 50% of the light produced in the phosphor screen is wasted in the current mammography screen-film technology. The proposed approach uses that light by exposing a second film which has similar film contrast, but, is faster than the first film, thereby permitting a wider exposure latitude imaging system without compromising image contrast. Two prototype screen-film combinations were developed. The test results demonstrated that, in addition to producing a breast image which is equivalent to the conventional screen-film method, the second film could provide enhanced diagnostic information for dense breast areas which are underexposed on the first film. The proposed technique could be the dominant approach to improve mammography in small hospitals for the next decade and provide cost-effective health care in the rural areas.

14. SUBJECT TERMS	15. NUMBER OF PAGES
Breast Cancer	26
	16. PRICE CODE

17. SECURITY CLASSIFICATION OF REPORT	18. SECURITY CLASSIFICATION OF THIS PAGE	19. SECURITY CLASSIFICATION OF ABSTRACT	20. LIMITATION OF ABSTRACT
Unclassified	Unclassified	Unclassified	Unlimited

FOREWORD

Opinions, interpretations, conclusions and recommendations are those of the author and are not necessarily endorsed by the U.S. Army.

____ Where copyrighted material is quoted, permission has been obtained to use such material.

____ Where material from documents designated for limited distribution is quoted, permission has been obtained to use the material.

__X__ Citations of commercial organizations and trade names in this report do not constitute an official Department of Army endorsement or approval of the products or services of these organizations.

____ In conducting research using animals, the investigator(s) adhered to the "Guide for the Care and Use of Laboratory Animals," prepared by the Committee on Care and Use of Laboratory Animals of the Institute of Laboratory Resources, National Research Council (NIH Publication No. 86-23, Revised 1985).

____ For the protection of human subjects, the investigator(s) adhered to policies of applicable Federal Law 45 CFR 46.

____ In conducting research utilizing recombinant DNA technology, the investigator(s) adhered to current guidelines promulgated by the National Institutes of Health.

____ In the conduct of research utilizing recombinant DNA, the investigator(s) adhered to the NIH Guidelines for Research Involving Recombinant DNA Molecules.

____ In the conduct of research involving hazardous organisms, the investigator(s) adhered to the CDC-NIH Guide for Biosafety in Microbiological and Biomedical Laboratories.

[signature] 8-24-98

PI - Signature Date

TABLE OF CONTENTS

Front Cover	1
Standard Form 298	2
Foreword	3
Table of Contents	4
1. Introduction	5
1.1. Notice of Discontinuation of the Grant	5
1.2. The Original Proposed Research	5
1.3. The Expanded Research Work	5
1.3.1. Purpose	6
1.3.2. Conventional screen-film mammography	6
1.3.3. Current approaches to improve breast cancer screening	6
1.3.4. Importance of the this work	7
2. Body	8
2.1. The prototype screen-film combinations	8
2.2. Characterization of the dual screen-dual film combination (Combination A)	10
2.2.1. Sensitometric response measurement	10
2.2.2. Digitized MTFs and limiting spatial resolution	12
2.2.3. Low contrast detectability	14
2.2.4. ACR accreditation phantom images	16
2.3. Characterization of the single screen-dual film combination (Combination B)	18
2.3.1. Characteristic Curve Measurement	18
2.3.2. Spatial resolution	18
2.3.3. Lesion detectability	19
2.4. Measurement results provided by Sterling Diagnostic Imaging, Inc.	20
3. Conclusion	23
4. References	24
List of Publications	26
Listing of Paid Personnel	26

1. INTRODUCTION

1.1. Notice of Discontinuation of the Grant

In April, 1998, the post-doctoral fellow, Zhenxue Jing, informed the University of Florida and USAMRMC to discontinue this funded support (Grant DAMD17-97-1-7067). The main reason was that the proposed research project was stalled due to some technical difficulties in making the metal loaded plastic scintillating fibers.

Since May, 1998, Dr. Zhenxue Jing has been working as a R&D Scientist for TREX Medical Corporation, LORAD Division, Danbury, CT.

1.2. The Original Proposed Research

The proposed work was focused on the development, optimization, and pre-clinical evaluation of a scanning slot x-ray detector for digital mammography. The primary goal was to optimize and finalize a plastic scintillating fiber screen (SFS) based scanning slot x-ray detector. The second effort was to compare the use of SFS with the use of a new CsI:Tl screen in a slot x-ray detector. The purpose was to optimize the x-ray detection material to develop a scanning slot x-ray detector with the best possible imaging performance for mammography. The final goal was to perform comparative receiver operating characteristic (ROC) analysis to evaluate the performance of the optimized scanning slot x-ray detector using an anthropomorphic breast phantom.

During the course of this project starting from June 1, 1997, the principle investigator and other colleagues have given a lot of effort to make plastic scintillating fibers with adequate metal loading. Unfortunately, those scintillating fibers made only generated very small amount of visible light under x-ray exposure levels typically encountered in mammography. It is likely that, when fibers were produced from a single metal loaded plastic scintilltor, the molecular structure integrity of the polymer and metal compounds was damaged due to heat or stretching. This damage directly reduces the efficiency of the plastic scintillating core materials to convert the absorbed x-ray energy into visible light.

The inability to successfully making metal loaded plastic scintillating fibers greatly devalued the merit of this research project. The NIH grant, which supported this project for the last three years, was expired at the beginning of this year. No further support was granted. As a result, the research work was essentially stopped.

1.3. The Expanded Research Work

During the one year period funded by USAMRMC, the principle investigator also conducted in parallel another research project which of great relevance to improving breast cancer detection in mammography. Dr. Jing was also the P.I. of this project, which was partially funded by a NIH SBIR grant to Nanoptics, Inc., Gainesville, FL. This document primarily reports the work and findings of the expanded research work.

1.3.1. Purpose

The general objective is to develop an improved screen-film mammography system which provides improved breast lesion detection in dense fibroglandular tissue without compromising diagnostic sensitivity for the "average" breasts.

1.3.2. Conventional screen-film mammography

Screen-film mammography is currently the only reliable means of detecting breast cancers in asymptomatic women [1-3]. Early detection with screening mammography has been shown to significantly reduce breast cancer mortality rates for women over age 50. Conventional mammography screen-film combinations are made of a single phosphor screen used as a back screen in combination with a single emulsion film.

There are several problems associated with the use of screen-film combinations which reduce the effectiveness of screening mammography [4-7]. Of these, the major technical limitation is related to the shape of the film's characteristic curves which necessitate a fundamental compromise between the film's display contrast and exposure latitude [8]. For screen-film combinations used in mammography, high film contrast is essential to detect subtle lesions with subject contrast in the order of ~1% [9]. As a result, the exposure latitudes of conventional mammography screen-film combinations are limited to about 40. However, typical film contrast is about 3.5 for film densities ranging from about 1.0 to 2.0, which only corresponds to a change in x-ray exposure by a factor of about two. Film contrast reduces quickly below the film optical density (O.D.) of 1.0 and above the film optical density of 2.0 [8], with film contrast values reduced to about 1.5 at film O.D. of 0.5 and 3.0.

This compromise in film contrast and exposure latitude is optimized to image compressed breasts of average thickness (~ 4.2 cm) and average density (~ 50% adipose and 50% glandular tissue composition). For thicker and dense breasts, x-ray exposure exiting a compressed breast can vary by a factor of 100 or greater [10]. Conventional mammography uses automatic exposure control (AEC) devices to produce a constant film optical density (~ 1.5) in some selected regions of the uniformly compressed breast region [11]. The film densities around the periphery of the compressed breast are typically much greater than 2.0 due to the excessive x-ray exposure to the screen-film cassette in these areas. Of more important concern are the dense breast regions which are frequently underexposed, and therefore, displayed with poor film contrast. In practice, between 30 to 60% of mammography screenings are performed on breasts composed at least partially of dense fibroglandular tissue [12]. It has been shown that the detection of a lesion surrounded by the dense fibroglandular tissue is more difficult than in a fatty tissue background [9]. Epidemiological studies also have shown that women with dense breasts are at increased risk of developing breast cancer [13,14]. The failure to detect lesions in the dense regions of the breast or in the dense breast is one of the major causes of missed early diagnosis of breast cancers [15,16]. Overcoming this problem is the principle objective of this work.

1.3.3. Current approaches to improve breast cancer screening

A number of innovative approaches have been investigated to overcome the problems associated with inadequate exposure latitude in screen-film mammography. Autoradiographic enhancement, blurred mask subtraction film printing, and electro-optical photographic equalization have been used to increase the contrast of underexposed regions of radiographic film [17-19]. However, these post-processing techniques suffer the inherit low contrast-to-noise ratio from the original images. In addition, these post-processing techniques also have the problems of reducing image resolution and increasing noise. X-ray exposure equalization by using tissue equivalent material to surround the breast and equalize the x-ray path length of the compressed breast [20] may not be practical due to the range of breast size encountered and the associated patient discomfort. By applying scanning equalization radiography to mammography, Sabol et al [21] have shown high film contrast could be achieved over the entire compressed breast. The problem is however the long time required to scan the whole breast which may result in patient motion and tube overheating.

A more advanced approach is digital mammography which has the potential to overcome many technical limitations of screen-film mammography. Digital imaging receptors typically have significantly wider exposure latitude than x-ray films and respond linearly to x-ray exposure over a wide range. Display contrast can easily be modified by digital manipulation. Digital mammography also enables digital archive, computer assisted diagnosis and remote diagnosis. A number of digital mammography systems have been developed and are currently under clinical evaluation [22-26]. These digital mammography systems have shown great promise in that they provide much higher detective quantum efficiency (DQE) and contrast sensitivity than screen-film mammography.

However, a major impediment to the wide application of digital mammography at present time is the limitation of display technology. The minimum requirement for image display is 4 k x 4 k at a pixel depth $\geq$12 bits. Current high resolution, adequately bright monitors only have a display size of about 2 k x 2 k, and are unable to provide, in a single image, the amount of information necessary for clinical diagnosis. Radiologists will have to view the full image at a reduced resolution and conduct a zoom and seek operation to view in detail a segment of the full image at a given time. In addition, current clinical practice requires breast images be compared in one reading session. For example, left vs. right and new vs. old comparisons require two or more images be displayed at the same time. It has been recognized that soft copy display of digital mammograms is not an acceptable method. Digital mammograms are being evaluated on printed laser films.

1.3.4. Importance of the this work

The proposed method overcomes the major technical limitation associated with breast cancer screening. Compared to conventional mammography screen-film combinations, this new method makes more efficient use of the scintillation light emitted in the phosphor screen and more efficient utilization of x-ray exposure to generate additional and important diagnostic information at no increase in patient radiation risk. The new method is especially useful to enhance earlier breast cancer detection in women with dense fibroglandular breasts. It has been shown that the

presence of extensive parenchymal densities is significantly associated with failure to detect breast cancer by mammography. In these cases, the mammographic features (such as masses and microcalcifications) have inherently low subject contrast and are frequently displayed with low film contrast due to film underexposure at these dense breast regions. The proposed methods can provide consistently high film contrast in dense regions of a breast image. The use of the proposed method has the potential to significantly improve the accuracy in early detection of breast cancer for women with dense breasts.

The National Cancer Institute (NCI) has accepted the recommendations on screening mammography of the National Cancer Advisory Board (NCAB), which recommended that NCI advise women 40 to 49 to get screening mammograms every one to two years if they are at average risk for breast cancer. In reaching its conclusions, NCAB considered updated findings from recent breast cancer screening studies which show that regular screening mammography of average risk women in their 40s reduces death from breast cancer by about 17%. In addition to the benefits of screening, NCAB also outlined the limitations of mammography which including (1) the larger number of false positives (~3 out of 10 women who begin annual screening at age 40) in breast cancer screening of women in their 40s; (2) due to the presence of dense breast tissue, up to 25% of all invasive breast cancers are not detected by mammography in women 40 to 49 years old compared with 10% of cancers for women in their 50s. With the recommended inclusion of this age group of women into screening populations, the percentage of dense breasts encountered in mammography screening will increase significantly. This could present significantly increased technical difficulties for current screen-film mammography systems. The proposed method could provide an immediate and cost-effective solution to the problems in imaging dense breasts. In addition, the proposed method can be used with existing mammography facilities at hospitals of any size, and, could provide cost-effective health care to all women including those in the rural areas.

2. BODY

2.1. The prototype screen-film combinations

Combination A

Figure 1 shows the cross sectional view of a prototype dual screen-dual film combination **(Combination A)**. Film #1 is a single emulsion film and is exposed by light emitted from the phosphor side of Screen #1. The geometry of Film #1/Screen #1 is the same as a conventional screen-film combination for mammography. Screen #1 is made of a Gd_2O_2S:Tb phosphor directly coated on a thin clear Mylar backing, which enables light to emit from this side of Screen #1. Film #2, sandwiched between Screen #1 backing and Screen #2, is a double emulsion film and exposed by light emitted from both screens. Screen #2 is also a Gd_2O_2S:Tb phosphor screen.

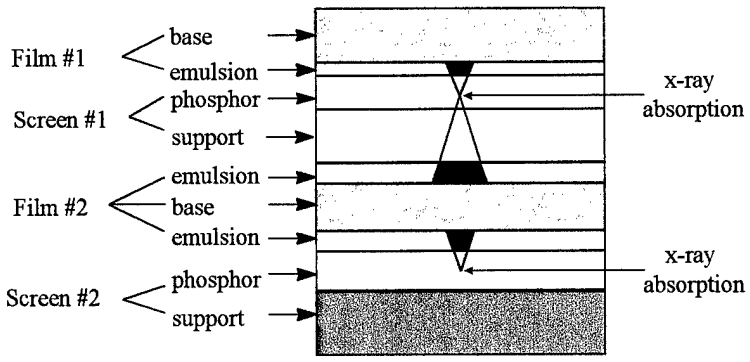

Figure 1. A dual screen-dual film combination. **(Combination A)**.

Table 1 summarizes the compositions of the films and screens for the dual screen-dual film combination used in this study. Film #1, Film #2, and Screen #2 are commercial products available from Eastman Kodak Company. Screen #1 was specially developed for this work by Eastman Kodak Company. Screen #2 does not have light absorbing dye in its phosphor, and a reflective backing was used to increase the light output.

Table 1. Summaries of film and screen compositions for **combination A** depicted in Figure 1.

Material	Compositions
Film #1	Kodak Min-R E film, single emulsion
Screen #1	Min-R phosphor (Gd_2O_2S:Tb, 34.0 mg/cm^2 coating weight) coated on a 4 mil clear Mylar sheet *
Film #2	Kodak T-Mat G (TMG) Film, double emulsion, no anti-crossover layer
Screen #2	Kodak Insight Multi-Exam (IME) screen (Gd_2O_2S:Tb, 43.0 mg/cm^2 coating weight, reflective backing)

* This screen was developed by Eastman Kodak Company for this project.

Combination B

Figure 2 shows the cross sectional view of a novel single screen-dual film combination **(Combination B)**. This combination is composed of one phosphor screen sandwiched between two single emulsion films. Light emitted toward the front of the screen is used to expose Film #1. Film #2, on the

other hand, is exposed by light emitted toward the back side of the screen. Table 2 summarizes the compositions of the films and screens for the single screen-dual film combination used in this study.

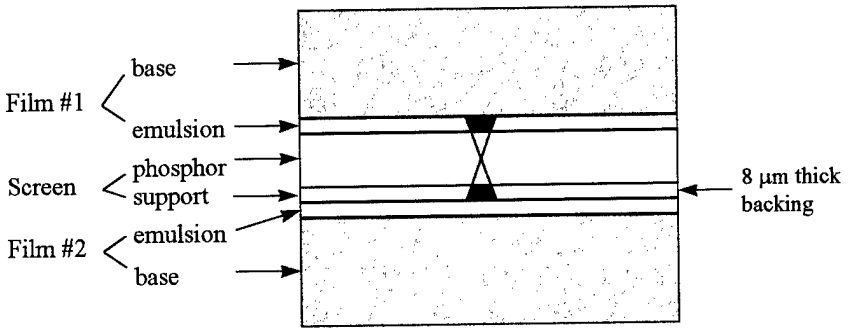

Figure 2. A single screen-dual film combination. **(Combination B)**.

Table 2. Summaries of film and screen compositions for **combination B** depicted in Figure 2.

Material	Compositions
Film #1	Kodak Min-R E film, single emulsion
Screen #1	Gd_2O_2S:Tb (27.2 mg/cm^2 coating weight) coated on a 8 μm thick proprietary polymeric sheet **
Film #2	Kodak Min-R H film, single emulsion

** This screen was developed by Sterling Diagnostic Imaging, Inc. for this project.

A conventional Kodak Min-R screen-Min-R E film combination was used as a standard for comparison. Each screen-film combination was loaded into a corresponding Kodak Min-R2 cassette. A GE Senograph 600t mammography x-ray unit was used to acquire all the images in this work. The x-ray tube has a molybdenum (Mo) anode and an added 0.03 mm Mo filter. A large focal spot size of 0.3 mm and a focal spot to screen-film cassette distance of 65 cm were used. All the films were developed in a Kodak X-Omat processor operating at 95°F and using extended processing cycles.

2.2. Characterization of the dual screen-dual film combination (Combination A)

2.2.1. Sensitometric response measurement

Sensitometric characterization of the prototype dual screen-dual film combinations was performed using a time-scale sensitometric method. For each x-ray tube potential (kVp) investigated, the dual screen-dual film cassette was uniformly exposed a number of times by varying mAs (i.e., the product of tube current and exposure time). X-ray exposures to the dual screen-dual film cassette were recorded, and the resultant film OD values were measured using a densitometer with a 2 mm aperture (Model 301, X-Rite Inc.).

Although not an optimum method in accurately characterizing the sensitometric response of a given screen-film combination[27], this time-scale sensitometric method is well suited to compare the relative sensitometric response of the two films in the prototype screen-film combinations. The relative responses of the two films are not affected by the film reciprocity-law failure because the two films are always exposed by the same x-ray exposure. In addition, this time-scale sensitometric method may be the most clinically relevant way to compare the two films in the dual screen-dual film combination.

Table 3 summarizes the measured x-ray exposures to the screen-film cassette to expose each film to an optical density value of 1.2. The relative speeds of the two films are also given in Table 3. The difference between the effective speeds of the two films is larger at the higher kVp. This is because a larger fraction of incident x-rays penetrates Screen #1 at the higher kVp. Relatively more x-rays are therefore absorbed by Screen #2 at the higher kVp. This increased x-ray absorption in Screen #2 produces more light, thereby increasing the effective speed of Film #2 relative to that of Film #1.

Table 3. Exposure required to reach film OD of 1.2. for Film #1, X_1, and Film #2, X_2. And the relative speed of Film #2 vs. Film #1, S, is given by $S = X_1/X_2$.

	Exposure (mR)		Relative Speed (S)
kVp	Film #1, X_1	Film #2, X_2	Film #2 vs. Film #1
25	9.10	4.30	2.12
28	8.07	3.56	2.27
30	7.60	2.85	2.67

Figure 3 shows the measured film OD values and the calculated film contrast as a function of x-ray exposure to the screen-film cassette for the dual screen-dual film combination at 28 kVp. The maximum film contrasts for Film #1 and Film #2 peak at about 14.8 mR and 5.7 mR, respectively. Currently, screen-film mammography typically produces a targeted film OD of ~1.5 using AEC. The corresponding exposure to the screen-film cassette is ~10 mR. Reducing this exposure level by a factor of two to ~5 mR, the Film #1 contrast decreases from ~3.3 (OD = 1.5) to ~2.2 (OD = 0.7). The corresponding Film #2 contrast at 5 mR exposure is ~3.3 (OD = 1.8). When exposure is further reduced to 3.8 mR, the Film #1 contrast decreases to ~1.6 (OD = 0.5). The corresponding Film #2 contrast is ~3.1 (OD = 1.25).

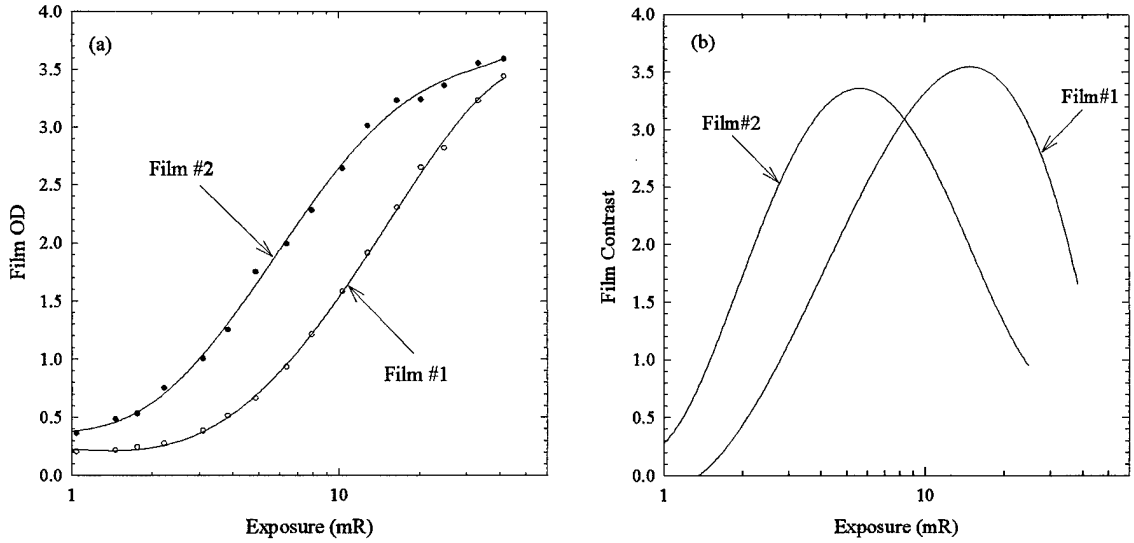

Figure 3. (a) Measured characteristic curves of the dual screen-dual film combination at 28 kVp; (b) Calculated film contrast as a function of x-ray exposure at 28 kVp. The base + fog densities are 0.18 and 0.21 for Film #1 and Film #2, respectively.

We have measured the film densities of underexposed areas on clinical breast images at two mammography centers. The resulting film densities were as low as ~0.4 on large dense areas of the breasts

for a significant number of cases. This finding is supported by the other previous studies [28,29]. It is therefore anticipated that a factor of two or greater improvement in film contrast can be achieved for dense areas of the breasts by the use of the dual screen-dual film combination.

Figure 4 shows the measured characteristic curves of the dual-screen-dual film combination and a standard mammography screen-film combination using the Kodak Min-R screen and Min-R E film. The film OD values were measured on the center of each step of an Aluminum step wedge image. The variations in x-ray exposures used to expose the dual-screen-dual film combination and the standard screen-film combination are measured to be less than 1%. The difference in speeds between Film #1 and the standard film is less than 10%. About 10% difference in speeds between two conventional screen-film cassettes frequently exists due to small variance in the phosphor coating weight and dye concentration. Therefore, Figure 4 demonstrates that there is negligible if any effect of light being reflected back on to Film #1 in the dual screen-dual film combination due to the use of a transparent Screen #1 backing.

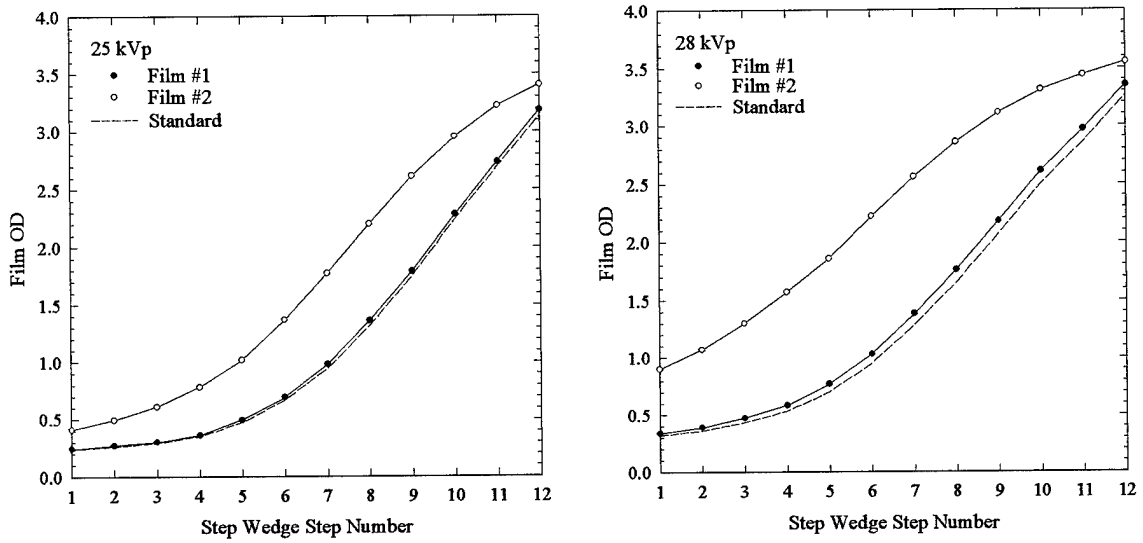

Figure 4. Measured characteristic curves of the dual-screen-dual film combination and a standard Kodak Min-R screen-Min-R E film combination at 25 and 28 kVp.

2.2.2. Digitized MTFs and limiting spatial resolution

Exploratory MTF measurements were performed to compare the differences in spatial resolution performance between Film #1 and Film #2, and between Film #1 and a Kodak Min-R screen-Min-R E film combination. Images of an edge object were acquired using the two screen-film combinations. The edge object was made of a Lead foil with 0.025 mm thickness. The films were subsequently digitized using a film digitizer with a 30 μm pixel size and 16 bit resolution. Edge spread functions (ESF) were obtained as the pixel intensity profiles across the digitized edges. MTF values were calculated from the Fourier transform of the line spread function (LSF), which was the differentiation of the corresponding ESF. These measurements of MTF provide reliable comparisons of the MTF performances between Film #1 vs. Film #2, and between Film #1 vs. standard in the spatial frequency range investigated. However, the results obtained are not true MTF values of the dual screen-dual film combination. The measurement of the sensitometric response of the dual screen-dual film combination by the standard inverse-square law method is under way. This measurement will allow the accurate analysis of the MTF of the dual screen-dual film combination[27].

Figure 5 shows the computed MTF curves from digitized edge images obtained at 28 kVp. The MTF of Film #1 is essentially the same as a Kodak Min-R screen-Min-R E film combination up to the limiting spatial resolution (16.67 lp/mm) of the film digitizer. The MTF curve of Film #2 displays two distinctive components, a quick drop in MTF values from 0 to ~5 lp/mm due to light spreading in the 4 mil thick Screen #1 backing, and an almost constant MTF value above ~8 lp/mm due to the sharp image signal generated from Screen #2. The purpose of this MTF measurement is to investigate the MTF performance of the Film #1 in comparison to a conventional screen-film combination (especially in the range o to 10 lp/mm), and the relative MTF performance of Film #2 to Film #1. These results are not to be taken as the true MTF values of the screen-film combinations studied. An accurate MTF measurement of the dual screen-dual film combination using the standard method will be pursued in the near future.

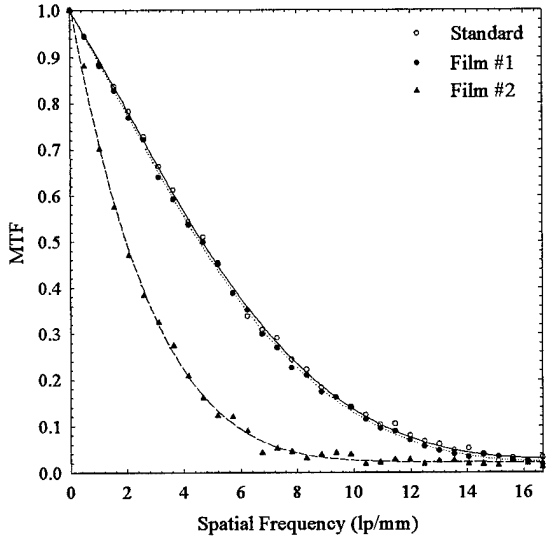

Figure 5. MTF curves measured from the digitized edge images obtained at 28 kVp. The edge object was a Lead foil of 0.025 mm thickness. Original edge images were digitized using a film digitizer with 30 μm pixel size and 16 bit resolution.

In addition, the images of a line pair resolution lead bar pattern (Model 07-539, Nuclear Associates, Carle Place, NY) were used to quantify the limiting spatial resolution performance of the dual screen-dual film combination. This test pattern contains resolution information up to 20 lp/mm. Table 4 summarizes the measured limiting spatial resolution as a function of the x-ray tube potential for the dual screen-dual film combination and a standard Kodak Min-R screen-Min-R E film combination. The limiting spatial resolution of Film #1 is >19 lp/mm and is comparable to that of a Min-R screen-Min-R E film combination. Film #2 limiting spatial resolution increases slightly from 10 lp/mm at 25 kVp to 11.5 lp/mm at 30 kVp.

Table 4. Measured limiting spatial resolution vs. kVp. The standard is a Kodak Min-R screen-Min-R E film combination.

X-ray tube potential (kVp)	Limiting spatial resolution (lp/mm)		
	Film #1	Film #2	Standard
25	19.5	10.0	20
28	19.5	11.0	20
30	19.5	11.5	20

A detailed investigation of the sources contributing to the image blur on Film #2 was carried out. Images of the same line pair resolution pattern were obtained for the following screen-film combinations: (1) A Min-R E film placed below the 4 mil thick backing side of Screen #1; (2) A Min-R E film placed above Screen #2; (3) A Kodak Insight IMG film replacing the TMG film in the dual screen-dual film combination. The IMG film is also a double emulsion film, but has an anti-crossover layer between its two emulsions. The measured limiting spatial resolutions are 7.5, 16.0, and 14.0 lp/mm for Combinations 1, 2, and 3, respectively. These results shows that light dispersion in the 4 mil thick Screen #1 back is a major source of image blur. Light crossover between the emulsions of the TMG film also decreases significantly the Film #2 resolution. A further improvement of Film #2 resolution can therefore be achieved by the use of a thinner Screen #1 backing and/or the used of a new Film #2 with the anti-crossover layer and with the satisfactory speed performance.

2.2.3. Low contrast detectability

A mammography contrast-detail (C-D) phantom (Model 180, GAMMEX RMI) was used to evaluate the low contrast visibility performance of the prototype dual screen-dual film combination. This phantom consists of a 15 cm x 11 cm x 1.5 cm thick Lucite base with protruding Lucite-disks of various thickness and diameter. In this study, the C-D phantom was placed on top of an additional 2.5 cm thick Lucite block, which formed a total phantom thickness of 4.0 cm. Images of the C-D phantom were generated with the use of a standard 5:1 ratio bucky grid. At 28 kVp, a total of six exposures were taken by varying x-ray exposure technique from 32 to 100 mAs. Figure 6 shows the Film #1 and Film #2 images of a C-D phantom placed on top of a 2.5 cm thick Lucite block. The x-ray exposure technique used was 50 mAs at 28 kVp.

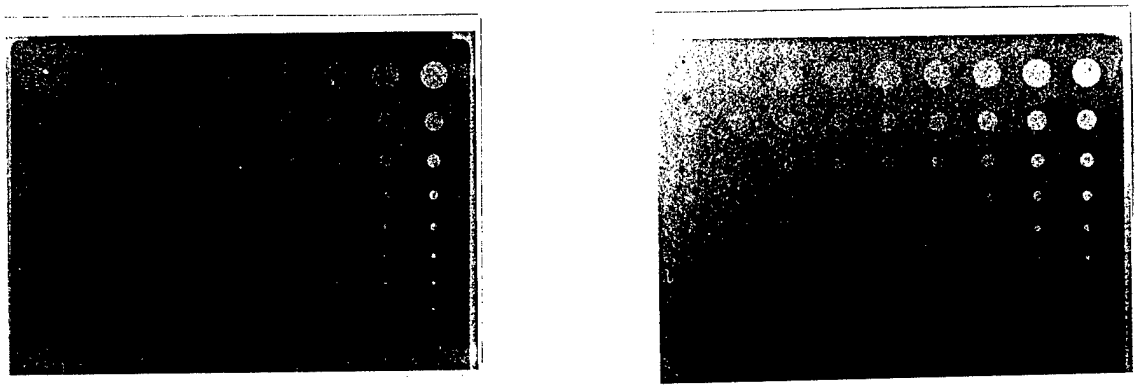

(a) (b)

Figure 6. X-ray images of a C-D phantom using an exposure technique of 28 kVp and 50 mAs with the use of a standard 5:1 grid for (a) Film #1 (OD = 0.56) and (b) Film #2 (OD = 1.46). The images were reduced to half of their original sizes during reproduction.

The resultant twelve films were read in random order under optimum viewing conditions by four readers (one physicist and three graduate students). The areas of the light box around the film was masked off to reduce glare and the room lights were also dimmed. The number of visible disks for each disk diameter was recorded. The use of a half score was allowed if the presence of a disk was in doubt. The threshold thickness and the corresponding threshold subject contrast was then calculated for each disk size, and plotted as a function of the x-ray exposure (mAs). The standard deviations on the threshold thicknesses were also calculated for the four observers.

Figure 7 shows the observed threshold disk thickness and the corresponding subject contrast as a function of the x-ray exposure (mAs) for four Lucite disk sizes ranging from 2.5 mm to 7.07 mm in diameter. The standard deviations in observed threshold thickness are also shown in Figure 7. For Film #1, the threshold contrast generally decreases by a factor of about two or greater when the x-ray exposure is reduced from 100 (OD = 1.30) to 32 mAs (OD = 0.34). These results are in broad agreement with Robson et al. [30] who performed a contrast detail study using a Kodak Min-R E/Min-R film/screen combination. Figure 7 also shows that the threshold contrast is up to a factor of two lower on Film #2 images when Film #1 is underexposed. This improvement in low contrast visibility is largest for the largest Lucite disks. The dependence of the observed threshold contrast on the x-ray exposure for the 5 mm diameter disk is consistent with the CNR measurement described later. These results suggest that small (<1 cm) breast lesions in typically underexposed dense breasts should be more easily detected with the dual screen-dual film combination.

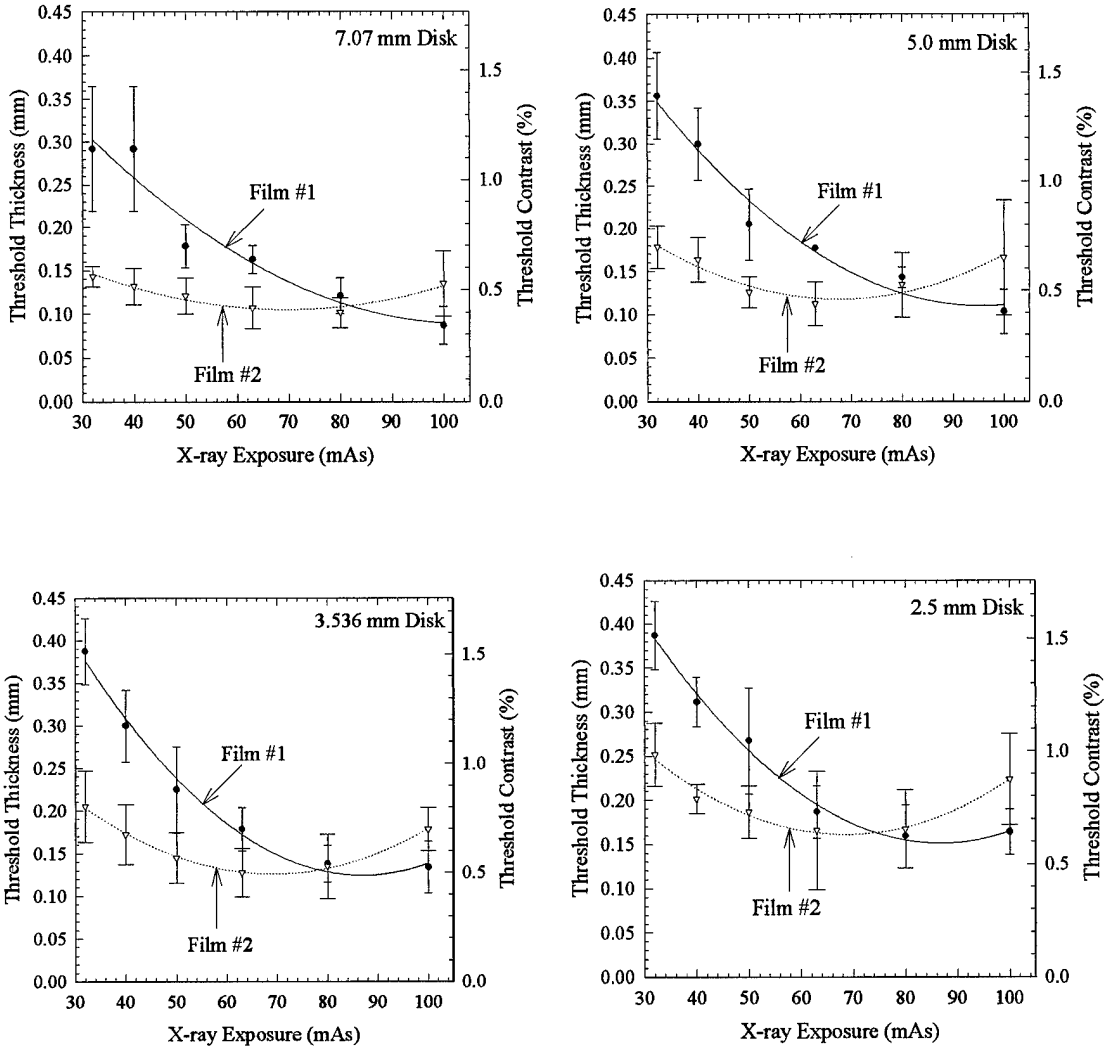

Figure 7. Observed threshold disk thickness and the corresponding subject contrast as a function of the x-ray exposure (mAs) for Lucite disk sizes of 2.5, 3.536, 5.0, and 7.07 mm in diameter at 28 kVp. Standard deviations in threshold thickness are also shown. The curves are second order polynomial fits.

In addition, a contrast-to-noise ratio (**CNR**) measurement was performed by digitizing the C-D phantom images using a 150 μm pixel size film digitizer. The digitized pixel intensities are proportional to the film OD values up to 3.0. The signal (***S***) was measured for a 5 mm diameter, 1.0 mm thick Lucite disk. The mean background intensity (***B***) and its standard deviation (σ) were calculated using measurements at the surrounding areas of this disk. The image contrast (***C***) was calculated as the difference between ***S*** and ***B***. **CNR** was then taken as the ratio of ***C*** to σ. The correlation between CNR and the observed threshold contrast was studied. Table 5 summarizes the measured film background OD, ***S***, ***B***, σ, ***C***, and **CNR**, for a 5 mm diameter, 1 mm thick Lucite disk on the images of Film #1 and Film #2. It is seen that Film #2 offers a factor of greater than two increase in image contrast for Film #1 images with OD less than 0.78.

Table 5. Film OD, digitized signal (***S***), mean background (***B***) and its standard deviation (σ), contrast (***C***) and CNR for Film #1 and Film #2. ***S*** values were measured for a 5 mm diameter, 1 mm thick Lucite disk on the films.

mAs	**Film #1**						**Film #2**					
(28 kVp)	***OD***	***S***	***B***	***σ***	***C***	***CNR***	***OD***	***S***	***B***	***σ***	***C***	***CNR***
32	0.34	294.6	326.6	6.2	32.0	5.16	0.86	781.1	853.5	11.6	72.4	6.24
40	0.44	397.2	430.6	7.6	33.4	4.40	1.16	1045.0	1145.7	14.8	100.7	6.80
50	0.56	524.5	571.1	8.6	46.6	5.42	1.46	1369.5	1472.4	14.9	102.9	6.91
63	0.78	720.4	798.0	13.0	77.6	5.97	1.83	1763.6	1878.3	15.3	114.7	7.50
80	1.04	986.8	1070.2	14.8	83.4	5.64	2.18	2147.8	2266.1	17.4	118.3	6.80
100	1.30	1276.0	1372	14.3	96.0	6.71	2.52	2532.1	2636.5	17.4	104.4	6.00

Table 5 also shows that the image noise level on Film #2 is always greater than that on the corresponding Film #1, which limits the improvement in CNR by Film #2 to an average of ~30% between 32 to 63 mAs. This higher level of image noise on Film #2 may be caused by the following two reasons: (1) The TMG film may have a higher granularity than the Min-R E film for the same film OD; (2) The light intensity emitted from the Screen #1 backing side is significantly less than that from the Screen #2 for the same amount of x-ray energy deposition. This difference in light emission could significantly increase the image noise as described by Swank [31]. A further investigation of the sources contributing to the Film #2 noise is therefore needed, and may enable a proper optimization to significantly reduce the Film #2 noise from its present level.

2.2.4. ACR accreditation phantom images

Figure 8 shows the ACR accreditation phantom (RMI 156) images which were obtained on Film #1 and Film #2 using an x-ray exposure technique of 25 kVp and 100 mAs. This phantom has a 4 cm thick Lucite base, and is embedded with nylon fibrils, tumor-like masses, and simulated microcalcifications. The background film OD is 0.51 for Film #1 and 1.27 for Film #2. This Film #1 image represents a typical clinical imaging problem when dense breast regions are underexposed. By the use of the prototype dual screen-dual film combination, the masses and fibrils are clearly better visualized on Film #2. Furthermore, there are about three groups of simulated microcalcifications which are visible on the Film #2 image. Therefore, the use of Film #2 also permits calcifications with sizes ~0.3 mm to be detected in this prototype **combination A**.

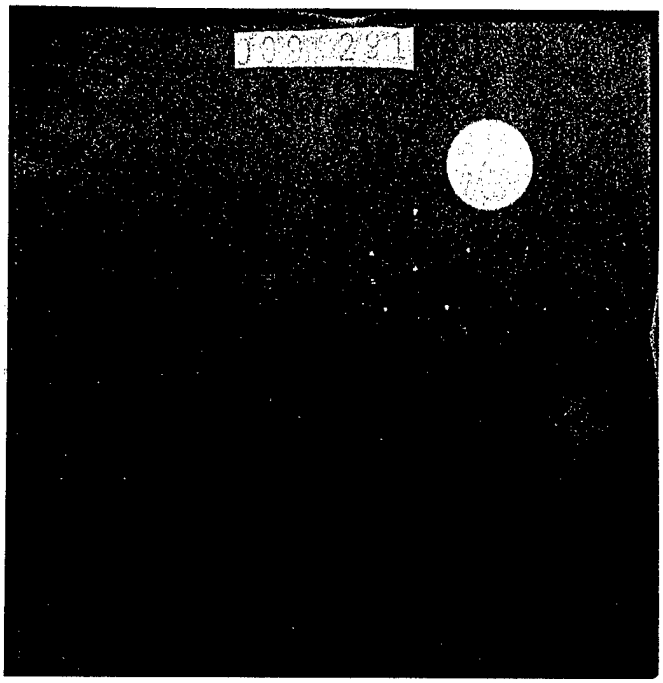

(a)

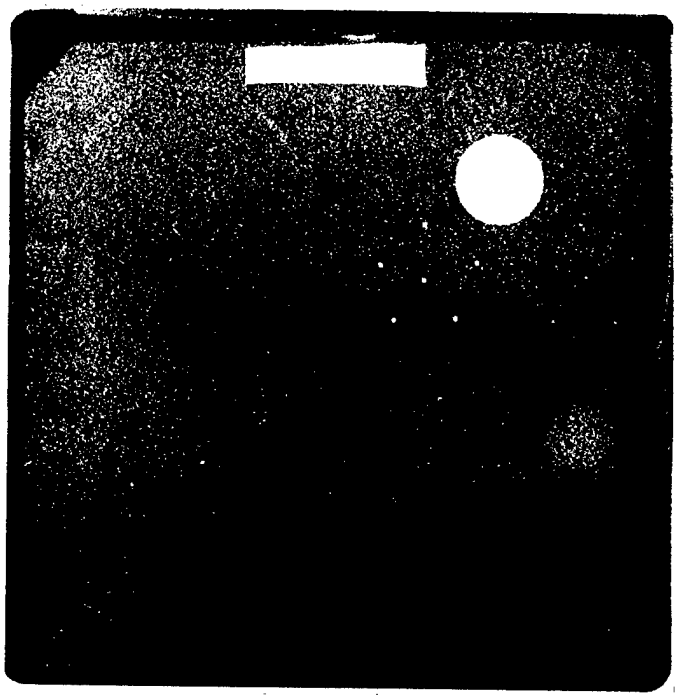

(b)

Figure 8. X-rays images of an ACR accreditation phantom obtained on (a) Film #1 and (b) Film #2 using an exposure technique of 25 kVp and 100 mAs with the use of a standard 5:1 grid. Film #1 OD is 0.51, Film #2 OD is 1.27. The images were reproduced from the original x-ray films without magnification.

2.3. Characterization of the single screen-dual film combination (Combination B)

2.3.1. Characteristic Curve Measurement

Images of an aluminum step wedge (built on the anthropomorphic breast phantom, each step is 0.01" thick) were obtained using the single screen-dual film combination (**B**). Figure 9 shows the measured film OD and the corresponding film contrast (defined as the difference in OD between two successive steps) as a function of step wedge number at x-ray tube potential of 26 KV. The film OD values were measured on the center of each step of the Aluminum step wedge image. Due to the extended processing condition, the Min-R H film has significantly improved film contrast. In the Film #1 OD range between ~0.5 to 0.7, Film #2 contrast is a factor of ~3 greater than Film #1.

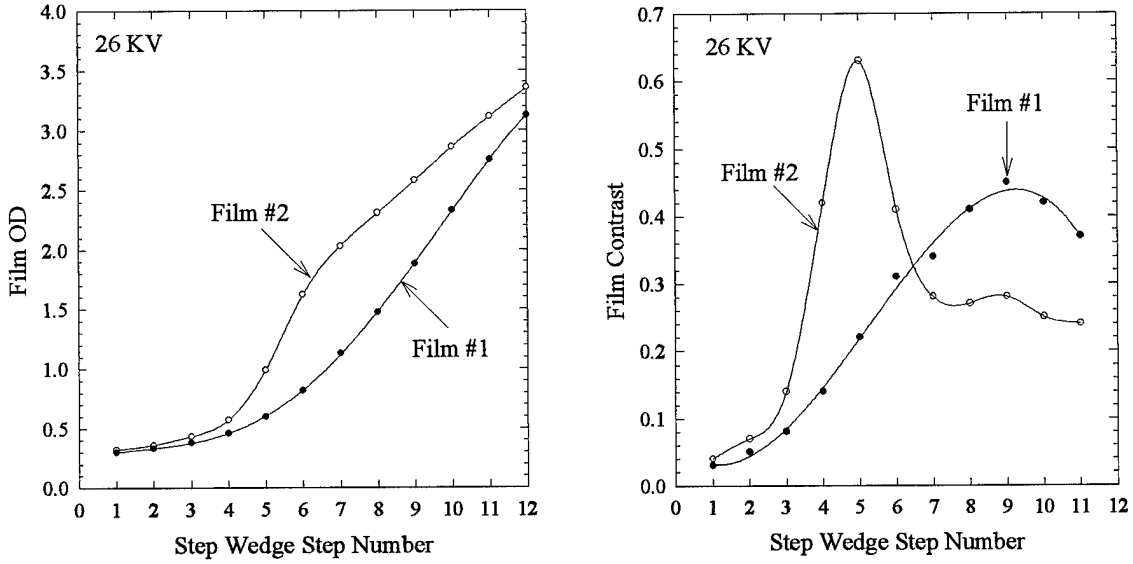

Figure 9. Measured characteristic curves and the corresponding film contrast of **combination B** at 26 kV.

2.3.2. Spatial resolution

Images of the lead resolution bar pattern were taken as before to obtain the limiting spatial resolution of the two films. Table 6 summarizes the measured limiting spatial resolution for **Combination B** at 26 and 28 kV. The >20 lp/mm limiting resolution on Film #1 is partly due to the 27.2 mg/cm^2 phosphor coating weight in the prototype screen, which is less than that (34.0 mg/cm^2) in the Min-R screen. As a result of the 8 μm thin screen backing, the limiting resolution of Film #2 is ~16 lp/mm

Table 6. Measured limiting spatial resolution for **combination B**.

X-ray tube potential (kVp)	Limiting spatial resolution (lp/mm)	
	Film #1	Film #2
26	>20	16.0
28	>20	16.5

2.3.3. Lesion detectability

Breast lesion detectability was investigated using the ACR accreditation phantom. First, images of the ACR accreditation phantom were acquired at 26 kV for **combination B** using an exposure technique of 100 mAs. Without changing the kV and mAs, additional Lucite blocks were then added on top of the accreditation phantom, and images of the resulting phantom were produced. The added Lucite block thickness ranged from 0.5 to 1.5 cm. These additional phantom images simulate the underexposed film images. The visibility of the embedded masses and microcalcifications on these images were evaluated by two physicists with experience in reading the ACR phantom images.

Figure 10 (a) shows the measured film background OD and the contrast of a 4 mm thick Lucite disc for combination B as a function of added Lucite block thickness at 26 kV. Figure 10 (b) shows the average number of masses and groups of microcalcifications observed on the ACR phantom images for **combination B** at 26 kV. It is seen that over the range where the contrast of the 4 mm Lucite disc is higher on Film #2 than Film #1, the visibility of masses is significantly improved on Film #2. Over the Film #1 OD range from ~0.5 to ~0.8, there is also a slight increase in the number of groups of microcalcifications seen on Film #2. The sizes of the microcalcifications in the 3rd and 4th groups are 0.32 mm and 0.24 mm, respectively. The improved visibility of microcalcifications and masses on Film #2 when Film #1 is underexposed has the potential to allow the detection of small microcalcifications and subtle lesions which may be masked by dense breast tissues.

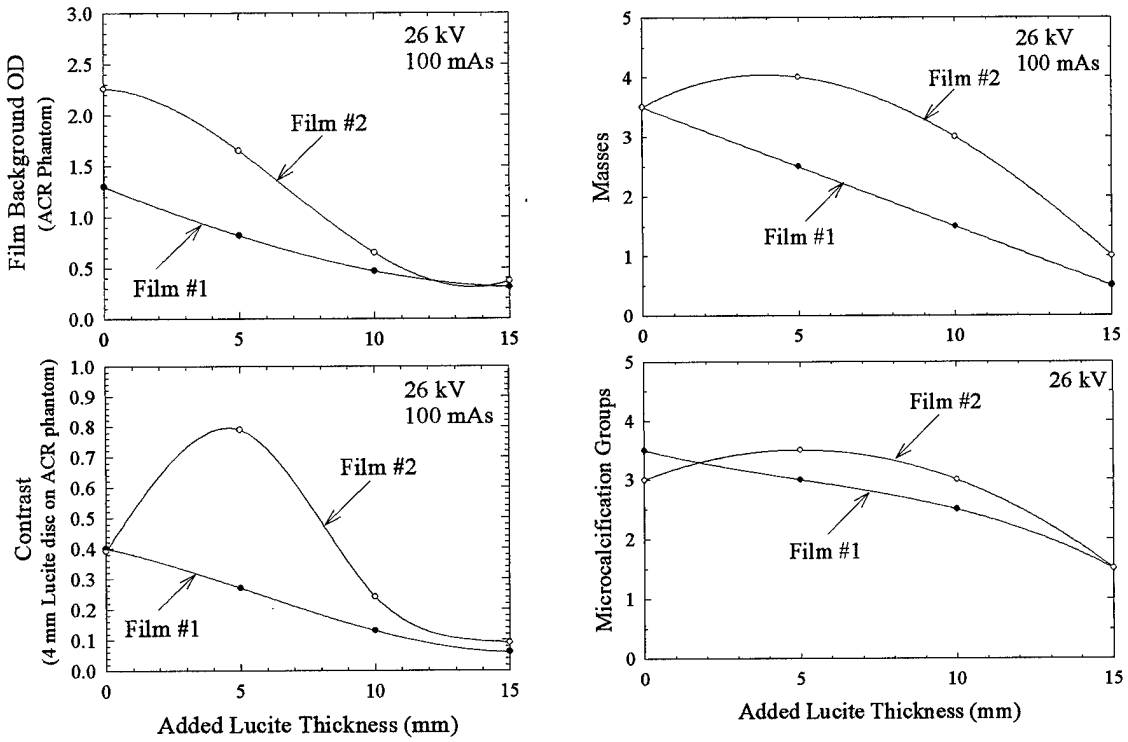

Figure 10. (a) Measured film background OD and the contrast of a 4 mm thick Lucite disc for combination B as a function of added Lucite block thickness at 26 kV; (b) The average number of masses and groups of microcalcifications observed on the ACR phantom images for **combination B** at 26 kV.

2.4. Measurement results provided by Sterling Diagnostic Imaging, Inc.

Based on the preliminary measurements performed, selected screen-film combinations as shown in Table 7 were further examined using specialized laboratory equipment at Sterling Diagnostic Imaging Inc.. **Combination 1** is the same as the **combination A** described above. However, all the films were processed using standard processing cycle for **combinations 1 to 3**.

Table 7. Summaries of screen-film combinations which were examined at Sterling Diagnostic Imaging, Inc.

Material	Combination 1	Combination 2	Combination 3
Film #1	Min-R E	Min-R E	Min-R E
	4 mil	8 μm	8 μm
Screen #1	transparent backing screen	transparent backing screen	transparent backing screen
Film #2	TMG	TMG	Min-R E
Screen #2	Insight ME	Insight ME	

Figure 11 shows the measured H&D curves for **combinations 1** and **2**. These curves were measured at 26 kVp using the standard x-ray wedge method which has been used by Sterling to measure its mammography screen-film combinations. The effective speed of Film #2 is a factor of 1.86 faster than Film #1 in **combination 1**. This result is consistent with our measurement shown in section 3.3.1. For **combination 2**, The effective speed of Film #2 is a factor of 2.51 faster than Film #1. This increased difference in **combination 2** is primarily due to the reduced screen #1 phosphor coating weight in the prototype 8 μm transparent backing screen in comparison with the phosphor coating weight of the prototype 4 mil transparent backing screen. Figure 11 also shows the H&D curve of Film #1 in **combination 1** is equivalent to that of a standard Kodak Min-R screen-Min-R E film used in this work for comparison. In **combination 2**, Film #1 is 66% faster than the standard. This difference is due to that the prototype screen #1 did not contain light absorbing dye, thereby producing more light output than the standard Min-R screen.

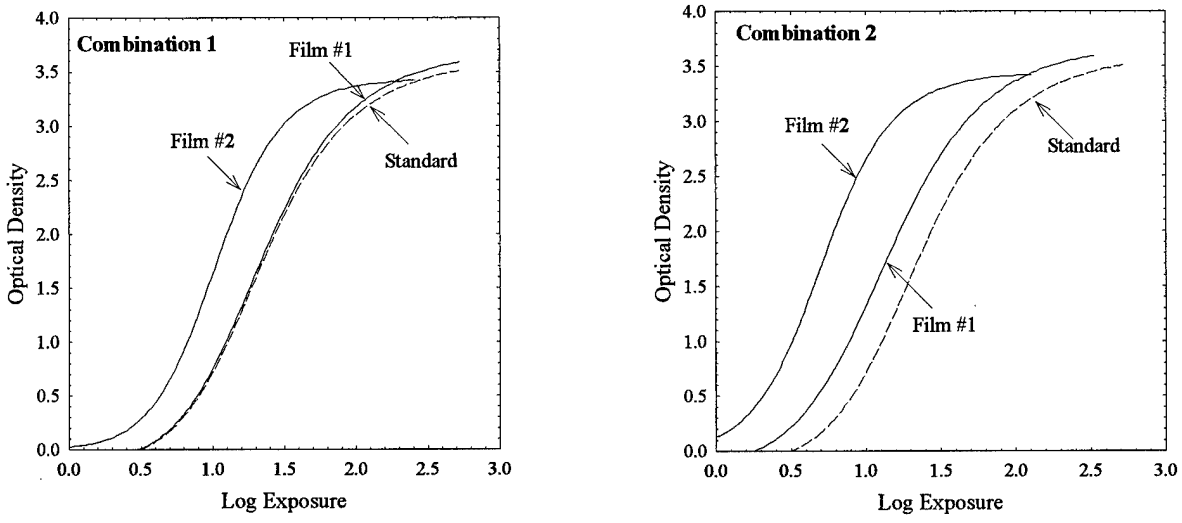

Figure 11. Measured H&D curves at 26 kVp. Standard was a H&D curve for a Kodak Min-R screen-Min-R E film combination measured in this work by Sterling.

Figure 12 shows the measured MTF curves for **combinations 1 to 3**. In **combination 1**, the MTF of Film #1 is better than those measured for two standard Kodak Min-R screen-Min-R E film combinations

at spatial frequencies up to ~13 lp/mm. However, this variation in MTF values can be observed in commercial screens due to manufacturing imperfection. It is concluded that the effect, if it exists, of the use of a transparent backing screen in the new screen-film combinations on reducing Film #1 resolution is negligible. MTF of Film #2 drops quickly to ~0.20 at 3 lp/mm.

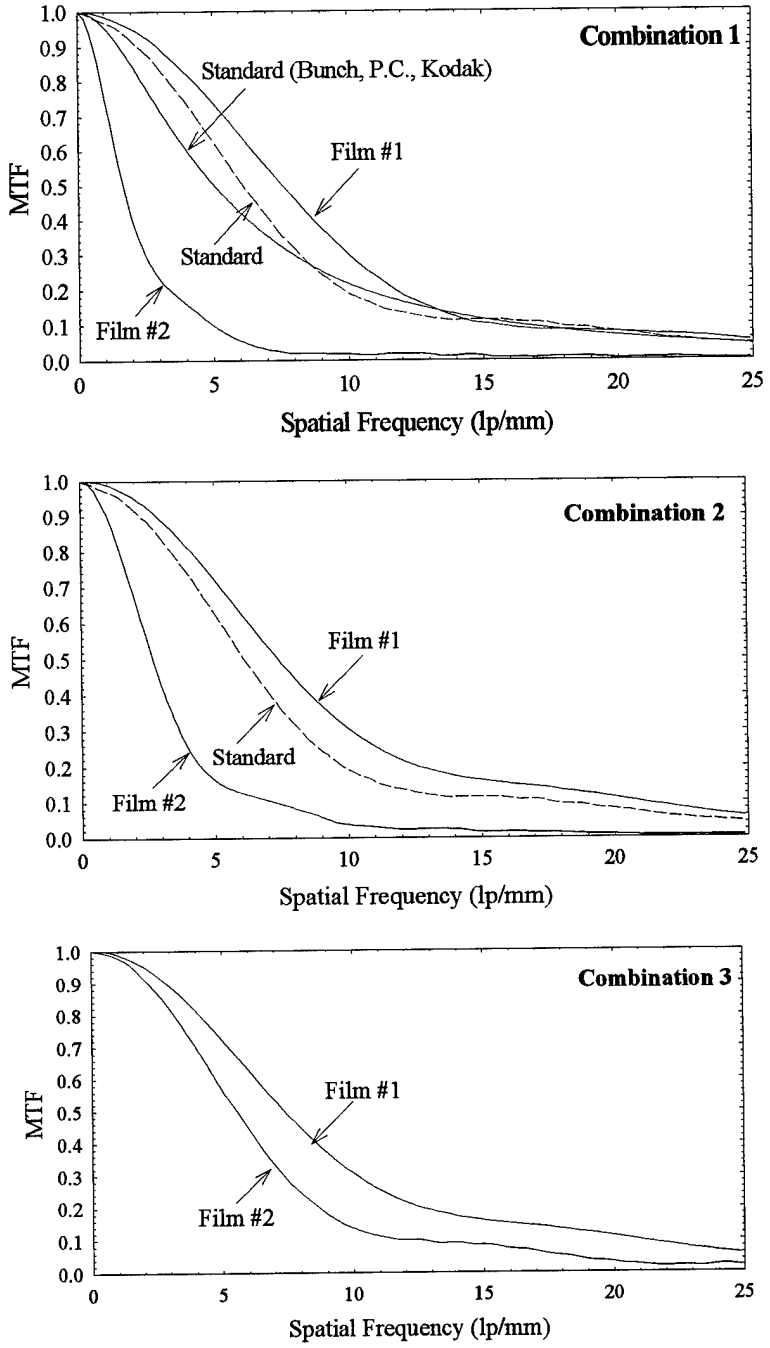

Figure 12. Measured MTF curves of the selected screen-film combinations. Standard was a MTF curve for a Kodak Min-R screen-Min-R E film combination measured in this work by Sterling. Measured data by Dr. Phillip C. Bunch of Eastman Kodak Company was also for a standard Kodak Min-R screen-Min-R E film combination provided to us by Dr. Bunch.

In **combination 2**, MTF of Film #1 is excellent again with values of ~0.70, 0.31, 0.16 and 0.11 at spatial frequencies of 5, 10,15 and 20 lp/mm, respectively. MTF values of Film #2 are ~0.41 at 3 lp/mm which is a significant improvement over **combination 1** due to the reduced screen #1 transparent backing thickness. In **combination 3** where the prototype 8 μm transparent backing screen was used in combination with two single emulsion films (Min-R E), MTF of Film #2 is excellent with values of 0.56, 0.14 and 0.09 at 5, 10, and 15 lp/mm.

The comparison between these MTF measurements shows that for a dual screen-dual film combination: (1) the use of thinner screen #1 transparent backing thickness improves Film #2 MTF, and (2) there is a significant reduction in Film #2 MTF due to light crossover between its emulsions. Two conclusions can be made from the data. The single screen-dual film combination can provide ≥15 lp/mm resolution in Film #2. The dual screen-dual film combination requires the use of double emulsion and anti-crossover technology in Film #2 to achieve high resolution. These results and findings are in agreement with the results shown in section 2.2.2.

3. CONCLUSIONS

The purpose of this work was to evaluate the feasibility of improving breast cancer screening of women with large and/or dense breasts using novel screen-film combinations which produce two images of the same compressed breast from a single x-ray exposure. During the one year period, the following work has been done:

1. Gd_2O_2S:Tb phosphor screens with transparent backing were developed. In particular, one screen was composed of regular Kodak Min-R phosphor (34.0 mg/cm^2 coating weight) coated on a 100 μm (4 mil) thick clear Mylar backing. Another screen made by Sterling Diagnostic Imaging has a phosphor coating weight of 27.2 mg/cm^2 and was coated on a 8 μm thick clear proprietary polymeric backing.
2. Two prototype screen-film combinations were designed. **Combination A** was a dual screen-dual film combination. **Combination B** was a single screen-dual film combination.
3. The measured characteristic curves and MTFs showed that Film #1 performances are comparable to a standard screen-film combination currently used in mammography. The measured limiting spatial resolution on Film #1 was 19.5 lp/mm.
4. Measurements of characteristic curves showed that Film #2 contrasts were >2x greater than Film #1 when Film #1 OD values were below 0.7 for a prototype dual screen-dual film combination.
5. Increased image contrast also lead to ~30% improvement in image signal-to-noise ratio (SNR) despite the existence of a high Film #2 image noise level.
6. The improved image SNR is evident in the observer performance study, which shows the threshold contrast in detecting small (<10 mm diameter) low contrast Lucite disks is up to a factor of two lower on Film #2 images when Film #1 is underexposed. This strongly suggests that low contrast breast lesions in dense tissue will be better detected using the new approach.
7. Limiting spatial resolution of the present Film #2 in **Combination A** is ~11 lp/mm, which can be markedly improved by the use of a thinner Screen #1 backing (100 μm was used) and/or a new film with anti-crossover technology. Limiting spatial resolution of Film #2 in **Combination B** is ~16 lp/mm.

In summary, the present work has demonstrated that the new screen-film combinations can provide a significant improvement in detecting small low contrast objects for typically underexposed film regions in screen-film mammography, and may be used by the radiologists to make more accurate diagnostic decisions in screening mammography.

4. REFERENCES

1. W. Zhou and R. Gordon, "Detection of Early Breast Cancer: An Overview and Future Prospects", Clinical Rev. in Biomedical Eng., Vol. 17, Issue 3, 203-255 (1989).
2. M. J. Yaffe, "Digital Mammography", Syllabus: A Categorical Course in Physics Technical Aspects of Breast Imaging Ed. by A.G. Haus and M.J. Yaffe, RSNA Publications, Il, 245-255 (1992)
3. A.G. Haus, "Recent Advances in Screen-Film Mammography", Radiologic Clinics of North America, Vo. 25, No. 5, 913-927 (1987)
4. Kuhn and W. Knupfer, "Imaging characteristics of different mammographic screens," Med. Phys. **19**, 449-457 (1992)
5. M. Nishikawa and M. J. Yaffe, "Signal-to-noise properties of mammographic film-screen systems", Med. Phys. **12**, 32-39 (1985)
6. G.T. Barnes, I. A. Brezovich "The intensity of scattered radiation in mammography", Radiology **126**, 1978, 243-247
7. Gary T. Barnes, "Mammography Equipment: Compression, Scatter Control, and Automatic Exposure Control", Syllabus: A Categorical Course in Physics Technical Aspects of Breast Imaging Ed. by A.G. Haus and M.J. Yaffe, RSNA Publications, Oakbrook, Il, 59-68 (1992)
8. Arthur G. Haus, "Screen-Film Image Receptors and Film Processing," Syllabus: A Categorical Course in Physics Technical Aspects of Breast Imaging Ed. by A.G. Haus and M.J. Yaffe, RSNA Publications, Oakbrook, Il, 69-84 (1992).
9. P. C. Johns, M. J. Yaffe, "X-ray characterisation of normal and neoplastic breast tissues", Phys. Med. Biol., 1987, Vol. 32, No. 6, 675-695
10. R. M. Nishikawa G. E. Mawdsley, A. Fenster and M. J. Yaffe, "Scanned-projection digital mammography", Med. Phys. **14**, 717-727 (1987).
11. C. Kimme-Smith, "Mammography screen-film selection, film exposure, and processing," In: G. T. Barnes, G. D. Frey, Eds. Screen film mammography: imaging considerations and medical physics responsibilities, Medical Physics Publishing, Madison, Wisconsin, 135-158 (1991).
12. G. H. Whitehouse and S. J. Leinster, "The variation of breast parenchymal patterns with age," Br. J. of Radiol. **50**, 315-318 (1985)
13. J. Brisson, F. Merletti, N. L. Sadowsky, J. A. Twaddle, A. S. Morrison, P. Cole, "Mammographic features of the breast and breast cancer risk," Am. J. Epidem. **115**, 428-437 (1982)
14. IH Gravelle, JC Bulstrode, RD Bulbrook, DY Wang, D. Allen, JL Hayward, "A prospective study of mammographic parenchymal patterns and risk of breast cancer," Br. J. Radiol. **58**, 487-491 (1986)
15. E. L. Schmitt and B. Threatt, "Tumor location and detectability in mammography screening," Am. J. Roentgenol. **139**, 761-765, (1982)
16. L. Ma, E. Fishell, B. Wright, W. Hanna, S. Allen, NF Boyd, "A controlled study of the factors associated with failure to detect breast cancer by mammography," J. Natl. Can. Inst. **84**, 781-785 (1992)
17. B. S. Askins, A. B. Brill, G. U. V. Rao, and G. , "Autographic enhancement of mammograms," Radiology **130**, 103-108 (1979)
18. M. B. McSweeny, P. Sprawls, and R. L. Egan, "Enhanced image mammography," Am. J. Roentgenol. **140**, 9-14 (1983)
19. R. A. Kruger, D. R. Reinecke, and R. L. "Light equalization mammography," Med. Phys. **17**, 696-700 (1990)
20. K. L. Lam and H-P Chan, "Effects of x-ray beam equalization in mammographic x-ray imaging," Med. Phys. **17**, 242-249 (1990)
21. J. M. Sabol, I. C. Soutar, and D. B. Plewes, "Mammographic scanning equalization radiography," Med. Phys. **20**, 1505-1515 (1993)

22. ADA. Maidment, MJ Yaffe, DB Plewes, GM Mawdsley, IC Soutar, "Imaging performance of a prototype scanned-slot digital mammography system", Proc. SPIE **1896**, 93-103 (1993)
23. Piccaro and E. Toker, "Development and evaluation of a CCD-based digital imaging system for mammography", in Electronic Imaging. SPIE X (Feb. 1993)
24. R. Fahrig, J.A. Rowlands, M.J. Yaffe, "X-ray imaging with amorphous selenium: Detective quantum efficiency of photoconductive receptors for digital mammography", Med. Phys. 22, 153-160 (1995)
25. JM Henry, MJ Yaffe, Bo Pi, J. Venzon, F. Augustine, TO Tumer, "Solid state x-ray detectors for digital mammography," SPIE Vol. 2432, 392-401, 1995.
26. D. B. Plewes, J. M. Sabol, I. Soutar, A. Chevrier, R. Shumak, "Role of equalisation mammography of dense breasts," Med. & Biol. Enrg. Comput. **33**, 167-173 (1995).
27. A. G. Haus, "Measures of screen-film performance," Radiographics 16, 1165-1181, 1996.
28. D. B. Plewes, J. M. Sabol, I. Soutar, A. Chevrier, R. Shumak, "Role of equalisation mammography of dense breasts," Med. & Biol. Enrg. Comput. 33, 167-173, 1995.
29. K. C. Young, M. G. Walls, and M. L. Ramsdale, "Mammography film density and detection of small breast cancers," Clinical Radiology 49, 461-465, 1994.
30. K. J. Robson, C. J. Kotre, and K. Faulkner, "The use of a contrast-detail test object in the optimization of optical density in mammography," *Br. J. of Radiol.* 68, 277-282, 1995.
31. R. K. Swank, "Absorption and noise in x-ray phosphors," *J. Appl. Phys.* 44, 4199-4203, 1973.
32. Dainty, J.C.; Shaw, R., Image Science, Academic, New York, 1974.
33. K. Kuhn and W. Knupfer, "Imaging characteristics of different mammographic screens," Med. Phys. 19 (2) 449-457 (1992).
34. R. M. Nishikawa and M. J. Yaffe, "Signal-to-noise properties of mammographic film-screen systems", Med. Phys. 12(1), 32-39 (1985).
35. C. E. Metz, "ROC Methodology in Radiologic Imaging", Invest. Radiol. 21, 720-733 (1986).
36. C. E. Metz, "Some Practical Issues of Experimental Design and Data Analysis in Radiological ROC studies", Invest. Radiol. 24. 234-245 (1989).
37. J. A. Hanley, "Receiver operating characteristic (ROC) methodology: The state of the art", Crit. Reviews Diag. Imaging 29, 307-335 (1989).
38. M. J. Yaffe, J. W. Byng, C. B. Caldwell, N. R. Bennett, "Anthropomorphic radiological phantoms for mammography", Medical Progress through Technology 19: 23-30, 1993.

List of Publications

1. Z. Jing, W. Huda, J. K. Walker, "Scattered Radiation in Scanning Slot Mammography," Medical Physics 25, 1111-1117, 1998.
2. Z. Jing, W. Huda, J. K. Walker, W. Y. Choi, "Detective quantum efficiency of a CsI:Tl scintillator based scanning slot x-ray detector for digital mammography," SPIE 3336, 583-591, 1998.
3. Z. Jing, J.K. Walker, "A novel dual screen-dual film combination for mammography," SPIE 3336, 572-582,1998.
4. W. Huda, A. Krol, Z. Jing, J. M. Boone, "Signal to noise ratio and radiation dose as function of photon energy in mammography," SPIE 3336, 355-363, 1998.

Listing of Paid Personnel

Zhenxue Jing, Ph.D.
Post-doctorate Fellow